Thermochimica Acta 506 (2010) 82–93

Contents lists available at ScienceDirect

Thermochimica Acta

journal homepage: www.elsevier.com/locate/tca

Thermoregulating response of cotton fabric containing microencapsulated phase change materials

F. Salaün[a,b,*], E. Devaux[a,b], S. Bourbigot[a,c], P. Rumeau[d]

[a] Univ Lille Nord de France, F-59000 Lille, France
[b] ENSAIT, GEMTEX, F-59100 Roubaix, France
[c] ENSCL, PERF, F-59650 Villeneuve d'scq, France
[d] IFTH, F-69134 ECULLY, France

ARTICLE INFO

Article history:
Received 25 February 2010
Received in revised form 23 April 2010
Accepted 27 April 2010
Available online 6 May 2010

Keywords:
Phase change materials
Microencapsulation
Coating
Thermoregulation
Textile

ABSTRACT

The purpose of this work is to manufacture a thermoregulating textile fabric based on the incorporation of melamine–formaldehyde microcapsules containing a n-alkane mixture. A series of fabrics containing different mass ratios of polyurethane binder to microcapsules were prepared by a padding process. This research was conducted to clarify the influence of the amount of microcapsules and binder on the thermal response using hot guarded plate, differential scanning calorimetry and hot disc measurements. MicroPCMs were incorporated into cotton fabric by using polyurethane binder without drastically modifying air permeability property. It was observed by DSC that the main endothermic peak of these composites was shifted to higher temperatures. The results indicate that the polymeric binder plays a main role during the 30 s of a cold to warm transition allowing to delay the temperature increase. Furthermore, the thermoregulating response depends on the surface deposited weight and the mass ratio binder to microcapsules. Thus, an interesting cooling effect is found for 20 g/m^2 of binder and from 40 g/m^2 of microPCMs. And a mass ratio binder to microPCMs taken between 1:2 and 1:4 is suitable to manufacture thermoregulating textile.

1. Introduction

Since the end of the 1980s, functional textiles have been developed to enhance textile performances according to the consumers' demand and to include a large range of properties with a higher added value. One of possible way to manufacture functional or intelligent textile products is the incorporation of microcapsules or the use of microencapsulation processes for textile finishing. Many of substances are encapsulated for potential textile applications [1–6]. One of these substances, phase change materials (PCMs), has been used to manufacture thermoregulated textiles to improve thermal comfort of the wearer [7]. PCMs are entrapped in a microcapsule of a few micrometers in diameter to protect them and to prevent their leakage during its liquid phase. These compounds possess the ability to absorb and store large amounts of latent heat during the heating process and release this energy during the cooling process.

The selection of a PCMs formulation depends typically on the required phase change temperature depending on end use. Indeed, PCMs should react to changes in temperature of both the body and the outer layer of the garment when they are incorporated in the textile substrate. Thus, for textile applications, PCMs with a phase change within the ambient temperature and comfort range of humans are suitable, i.e. in a temperature range from 18 °C to 35 °C. To avoid any liquid PCMs diffusion within a fibrous substrate, these compounds need to be contained in a capsule. At the current state of the microencapsulation technology, the choice of suitable PCMs for the manufacture of a textile containing microencapsulated PCMs was restricted to n-alkane. Furthermore, paraffin waxes were preferred due to their high latent heat, and they are chemically inert, non-toxic, non-corrosive and non-hygroscopic. Thus, n-eicosane [8], n-octodecane [8–16] and n-hexadecane [8,9,11] are the most PCMs chosen to be applied. In these studies, pure compound was used as PCM material and therefore the phase change occurs in a narrow temperature change at the melting temperature of the n-alkane. The use of binary mixture of n-alkanes allows to adjust the melting point (or phase change temperature) by modifying the composition, that also leads to a decrease in the overall latent heat of fusion [17]. Furthermore, some of the binary mixture, i.e. hexadecane/octadecane [18], octadecane/hexadecane [18], or tetradecane/hexadecane [19] have a solid/liquid or a solid/solid transition which takes place in a relatively narrow temperature change. The use of the binary mixture of hexadecane/eicosane

* Corresponding author at: ENSAIT, GEMTEX, F-59100 Roubaix, France. Tel.: +33 3 20 25 64 59; fax: +33 3 20 27 25 97.
E-mail address: fabien.salaun@ensait.fr (F. Salaün).

0040-6031/$ – see front matter © 2010 Elsevier B.V. All rights reserved.
doi:10.1016/j.tca.2010.04.020

allows to widen this temperature change and can be suitable for textiles application [20,21]. Nevertheless, this widening is accompanied by a decrease of the latent heat which can be caused by the formation of a concentration distribution in the liquid film due to small scale segregation [17].

The binary mixture of n-hexadecane/n-eicosane was also studied by Sarier and Onder [8], they concluded that to enhance the thermal capacity of fabrics it should be better to use a combination of microcapsules containing different types of PCMs rather than those including a mixture of them. They have observed that the mixture was satisfactory to provide a buffering effect against temperature changes and to regulate the temperature at the target of desired value. In fact, the main problem to design a thermoregulated textile is to define which kind of PCM should be incorporated onto each layer of fabric.

The step of encapsulation allows to manufacture textile containing microcapsules by various ways to fix the microcapsules within the fiber structure permanently, to embed them into a binder or to mixed them into foam [7,22]. They will remain thermally effective as long as the coating or the fibers stay intact [23]. The incorporation of PCMs into the matrix of artificial or synthetic fibers can be achieved either by wet spinning for e.g. polyacrylonitrile [24,25], polyacrylonitrile–vinylidene chloride [15], acrylic fiber [26], or by melt spinning [27] for polypropylene [28] or polyethylene fiber [15]. Although, the touch, drape, softness and color were not modified by the spinning process, the thermal heat capacity of the obtained fiber was limited to a low microPCMs loading content (5–10%). Moreover, the processing conditions may damage the microcapsules shell and the formation of clusters of particles can alter the thermo-mechanical properties of the fibers. The application of a foam pad allows the incorporation of greater amount of microcapsules and to realize a mixture of different PCMs to give a wide range of regulation temperature. These composites containing microPCMs in the range from 20% to 60% by weight were found to be leak-resistant with enhanced thermal properties [11,29,30]. The third way investigated to apply microPCMs to fabric is all common coating process [31–33], such as knife over roll [31,34], screen printing [10,35], pad-dry-cure [33], knife over air, and gravure and dip coating [36,37]. The method for manufacturing coating composition was widely described in the patent literature, nevertheless few papers published in the literature give account of the formulation of coating, finishing of fabrics and therefore the evaluation of their characteristics more specially thermal and durability properties [16,37]. The choice of the conditions process influences the microencapsulated fabric behaviour and the yield [38]. Thus, Choi et al. [10] have observed that the heat capacity of the microencapsulated fabrics decreased as the curing temperature increased. Furthermore, the efficiency of a binder to link microcapsules on a textile surface depends on the compatibility of the different interfaces of the products involved by the coating process. The choice of a binder adapted to the microcapsules can be determined by the comparison of the surface energy components induced by the contact angle measurement method and washing tests [39]. In our previous work, we have found that a polyurethane based binder was the most suitable to link melamine–formaldehyde microcapsules [39]. Furthermore, the adhesion of microcapsules was closely dependent on the chemical nature and structure of the textile support. Nevertheless, the use of polymeric binds presents some drawbacks, since the incorporated amount should be enough to obtain permanent linkage which can alter the fabric properties such as drape, air permeability, breathability, thermal resistance, softness and tensile strength can be affected adversely as the percentage of binder add-on increases. Thus, Pushaw [30] have reported the difficulties to maintain durability, moisture vapour permeability, elasticity and softness of coated fabrics when the coating was loaded with a sufficiently high content of microPCMs. However, the influence of binder/microPCMs ratio on thermal capacity of thermoregulating fabric has not been reported in detail.

In this study, we intended to report on how to manufacture a thermoregulating textile containing microPCMs applied by a coating technique.

The first aim was to determine the influence of the binder concentration in the mixing ratio of binder and microcapsules on the formation and the thermal behaviour of binder/microPCMs composite by scanning electron microscopy (SEM), and differential scanning calorimetry (DSC) analysis. Prior their incorporation, the surface morphology, chemical structure and thermal properties of microcapsules were investigated using scanning electron microscope (SEM), Fourier-transform infrared spectroscope (FT-IR), and DSC, respectively. Second, thermal properties, i.e. thermal resistance, thermal conductivity and thermal storage/release properties, were also investigated by hot-disk measurement and using a guarded hot plate inside environmental chambers to find out the enhanced buffering effect of the fabric.

2. Experimental

2.1. Materials

n-Hexadecane ($C_{16}H_{34}$), n-eicosane ($C_{20}H_{42}$) and tetraethyl orthosilicate ($Si(OC_2H_5)_4$) (TEOS) used as PCMs formulation were purchased from Acros organics and used as core material. Arkofix NM used as shell-forming was kindly supplied by Clariant (France). Arkofix NM is a melamine–formaldehyde precondensate in aqueous solution (68 wt.%). Nonionic surfactants, Tween 20 and Brij 35 (Acros Organics) were used as emulsifiers. For pH control, triethanolamine and citric acid were used (Aldrich). The commercial binder used in this study was Dicrylan PMC (polyurethane from Ciba Specialty Chemicals).

A 100% cotton fabric (566 dtex warp and 564 dtex weft yarns at densities of 26 ends/cm × 16 picks/cm, weighing 270 g/m^2, thickness of 0.50 mm), labelled COTTON, was chosen as the specimen.

2.2. Preparation of the microcapsules

The preparation of the microcapsules was carried out in an IKA Labor Pilot 2000/4 machine equipped with a mechanical stirrer via an *in situ* polymerization according to the method described previously [20]. Two solutions were prepared separately. In solution I, 100 g of Brij 35, 100 g of Tween 20 and 630 g of Arkofix NM were dissolved in 2200 mL of distilled water. The solution I was adjusted to pH 4 with 10.0 wt.% citric acid solution. In solution II, 480 g of n-hexadecane, 480 g of n-eicosane and 40 g of TEOS were mixed in a 2000 mL beaker at 40 °C. Solution II was poured into the reactor containing the solution I under stirring at 10 000 or 13 500 rpm during 20 min at 50 °C. The stirring speed was decreased to 400 rpm with an anchor stirrer after 20 min. The reaction system was kept at the stirring state for 4 h at 55 °C. Then the pH of the solution was adjusted to 9 with 50 wt.% triethanolamine solution to complete the reaction. After 30 min of continuous agitation, the regulation batch and the stirrer were switched off. Once cooled to room temperature, the suspension of microcapsules was collected.

2.3. Binder/microPCMs composite film preparation

To compare and examine the influence of binder/microPCMs ratio on the morphological observations and thermal properties of the composite, solution cast film were also prepared. 10 films were cast by making a binary mixture of binder at various concentrations (from 10 to 100 wt.%) and microPCMs. This solution was cast in a Teflon mold and then placed in an oven at 100 °C for 4 min to ensure

Table 1
Textile specimens prepared and their specifications and properties.

Specimen	Weight deposited[a] (g/m^2)	Add-on (%)	$Mass_{binder}$ to $mass_{microPCM}$ ratio
COTref	–	–	–
COT1/0-(54)	54	20.0	1:0
COT1/0-(64)	64	23.7	1:0
COT1/0-(81)	81	30.0	1:0
COT4/1-(49)	49	18.1	4:1
COT3/2-(29)	29	10.7	3:2
COT3/2-(40)	40	14.8	3:2
COT3/2-(62)	62	23.0	3:2
COT2/3-(46)	46	17.0	2:3
COT1/2-(17)	17	6.3	1:2
COT1/4-(17)	17	6.3	1:4
COT1/4-(102)	102	37.8	1:4
COT0/1-(210)	210	77.8	0:1

[a] Weight deposited = total amount of binder + MPCM deposited on each fabric.

complete removal of water and subsequently at 150 °C for 4 min to obtain a crosslinked composite.

2.4. MicroPCMs coating on textile substrate

The textile impregnation of the cotton fabric was made under the different baths containing the binder and the microcapsules at different concentrations (Table 1). It has been carried by immersion of the fabric at 2 m/min in the different formulation baths. Once impregnated, the samples were pressed by a BENZ vat padding device without pressure in order to keep the microcapsules intact. Then the drying treatment step was done in a BENZ frame under ventilation at 0.5 m/min speed during 4 min at 100 °C (to evaporate the water) and 4 min at 150 °C (to insure adequate binder crosslinking). The add-ons for treated fabrics were calculated according to Eq. (1):

$$\text{Add-on}\,(\%) = \frac{a-b}{a} \quad (1)$$

where a is the weight of specimen after treating, and b, the weight of specimen before treating.

2.5. Analytical methods

2.5.1. DSC measurements

The thermal behaviour of the binder and the microparticles was recorded using a TA instrument type DSC 2920 piloted on PC with TA Advantage control software. Indium was used as standard for temperature calibration and the analysis was made under a constant stream of nitrogen. Samples were placed in aluminum pans which were hermetically sealed before being placed on the calorimeter thermocouples. The sample space was purged with nitrogen at a constant flow (50 mL min^{-1}) during the experiments. Transition temperatures and enthalpies were obtained from a least four independent experiments on 4.0 ± 0.1 mg samples with a scanning speed of 2 K min^{-1}.

The specific heat of n-alkanes formulation was a constant in the measured temperature range. The content of PCMs in the microcapsules can be estimated according to the measured enthalpy:

$$\text{PCMs content} = \frac{\Delta H_{\text{PCM in microcapsules}}}{\Delta H_{\text{PCMs}}} \times 100 \quad (2)$$

where $\Delta H_{\text{PCM in microcapsules}}$ and ΔH_{PCMs} are the melting enthalpy of PCMs in microcapsules and the binary mixture of n-alkanes formulation (PCMs formulation), respectively.

In order to determine the thermal stability of the reversible phenomena of phase change, the microcapsules were subjected to repeated cycles of melting and crystallization by increasing the isothermal temperature of 10 °C at each test. The temperature rose and fell at 10 K min^{-1}. The explored temperature range was chosen in order to take all possible phase changes into account, and the enthalpies were measured between −15 °C and 45 °C. Furthermore, standard two-hole vented pan covers were used for this test.

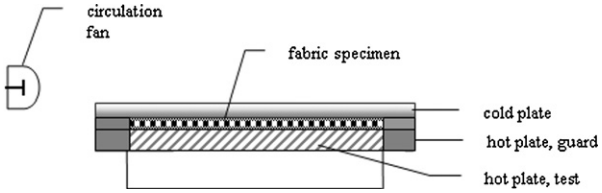

Fig. 1. Schematic diagram of guarded hot plate apparatus.

2.5.2. Microscopic examinations

The microcapsules and the binder/microcapsules composites surface morphologies were observed with optical microscopy (Axioskos Zeiss) equipped with a camera (IVC 800 12S) and with electronic scanning microscopy (Philips XL 30 ESEM) (SEM). SEM was also used to check the presence of the microcapsules and their dispersion into the textile.

2.5.3. Hot disk

The thermal conductivities of fabrics containing microcapsules were measured by the hot-disk method thermal analyzer (TDA-501). The hot-disk method utilizes a thin disk-shaped sensor (hot-disk sensor) to measure thermal conductivity. The measurement time was kept at 20 s, and the output power to the hot-disk sensor was set to 40 mW. The sensor radius was 3.189 mm. At least five measurements were performed for each material to ensure the repeatability of the results. During the measurement, the hot-disk sensor was sandwiched between the two samples.

2.5.4. Guarded hot plate apparatus

Since, there is no standard method for measuring the thermal regulating properties of heat-storage and thermoregulated textiles and clothings, we choose to use a protocol test developed at the French Institute of Clothing Textiles (IFTH, Lyon).

The test apparatus consisted of a guarded hot plate assembly enclosed in a climatic chamber (32 °C, air speed was 1 m/s) (Fig. 1). The device consists of a plate heated to a constant temperature matching the human skin temperature, i.e. 35 °C. The test section is in the centre of the plate, surrounded by the guard and lateral heater that prevents heat leakage. The fabric sample is placed on the plate surface and the heat flux from the plate to the environment is measured. Once the specimen was placed onto a heating plate and covered by a cold plate (at 8 °C, 11 °C or 13 °C) until it reached a stationary state. Then, the cold plate was pulled off to generate a temperature gradient through the fabric. The changes of surface temperature and heat loss of the hot plate are then recorded and used to characterize the thermal regulatory properties of the PCM fabrics.

For the determination of thermal resistance of the sample, the air temperature was set to 20 °C and the relative humidity was controlled at 65%. Air speed generated by the air flow hood was set to 1 ± 0.05 m/s. After the system reached steady state, total thermal resistance of the fabric was calculated using (Eq. (3)):

$$R_{ct} = A\frac{T_s - T_a}{Q} \quad (3)$$

where R_{ct} (m^2 K W^{-1}) is the total thermal resistance of fabrics plus the boundary air layer, A the area of the test section (m^2), T_s the surface temperature of the plate (K), T_a the temperature of the ambient air (K), and Q the electrical power (W).

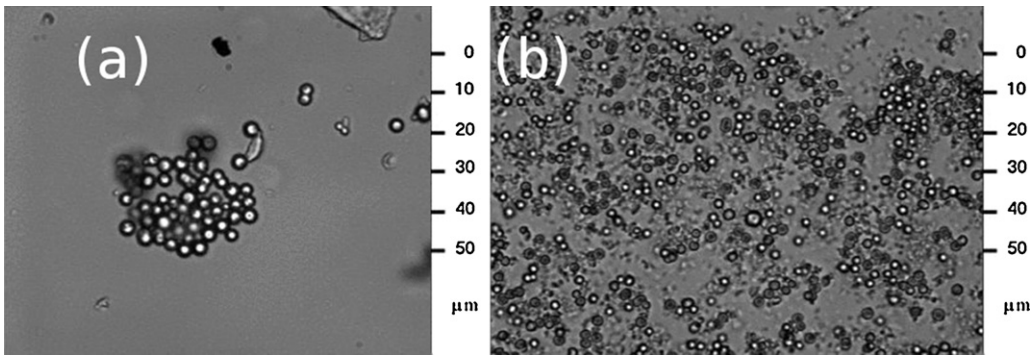

Fig. 2. Optical micrographs (64×) of microcapsules obtained with a stirring rate of 10 000 (a) and 13 500 (b) rpm, respectively.

2.5.5. Air permeability

The air permeability of textile fabrics is determined by the rate of flow of air passing perpendicularly through a given area of fabric is measured at a given pressure difference across the fabric test area over a given time period. Transverse air permeability was measured with FX3300 (Textest, Switzerland) with a pressure applied of 196 Pa, according to ISO 9237 [40].

3. Results and discussion

3.1. Microencapsulation of a n-hexadecane/n-eicosane binary mixture

Before examining the thermal properties of the fabrics, we focus on the chemical and thermal characteristics of the microPCMs synthesized from an *in situ* polymerization to determine the optimum treatment conditions to coat them.

The formation of microcapsules containing phase change materials occurs in four consecutive steps. The first step is the liquid/liquid dispersion of binary mixture of n-hexadecane/n-eicosane in continuous phase containing the amino pre-polymers, surfactant and water at pH 4. The dispersion of the binary mixture of n-hexadecane and n-eicosane in the continuous phase is the determining step in establishing the size distribution of the final particles, having the desired physical properties. Thus, from the results obtained in the laboratory scale study [43], the pH was adjusted during the emulsion step to 4 to reduce surface tension of the continuous phase, which allows the reduction of intermolecular distances between surfactant molecules, and therefore leading to enhanced emulsification. The phase volume ratio of the dispersed organic phase to the continuous phase was fixed to 0.42 to obtain narrow size distribution and a mean diameter of the dispersed particles within the range from 1 to 2 µm after 20 min of stirring (Fig. 2).

3.1.1. Structure of microPCMs

The FT-IR spectra of n-hexadecane and n-eicosane binary mixture (a), melamine–formaldehyde shell (b) and microcapsules (c) are presented in Fig. 3 to allow the identification of various core and shell microcapsules via known characteristic wavenumbers. According to the FT-IR spectra (Fig. 3), hydroxyl, imino and amino stretchings are located on both sides of 3370 cm^{-1} in the spectra of the microcapsule shell and microencapsulated PCMs (b and c). As seen in the figure, the spectra (a) and (c) show also a strong absorption band at 2952–2823 cm^{-1} associated with the aliphatic C–H stretching vibrations of the n-alkanes. Furthermore, the in-plane rocking vibration of the CH_2 groups is observed at 717 cm^{-1}, and C–H bending vibration in CH_2 is found at 1468 cm^{-1} and 1368 cm^{-1}. Additional characteristic absorption bands of melamine–formaldehyde resin appear at 1550 cm^{-1} and 1488 cm^{-1} due to the C–N multiple stretchings in the triazine ring. Characteristic triazine ring bending at 810 cm^{-1} can also be observed. On the one hand, C–H bending vibration in CH_2 is found at 1483 cm^{-1} and 1371 cm^{-1} due to methylene bridges. On the other

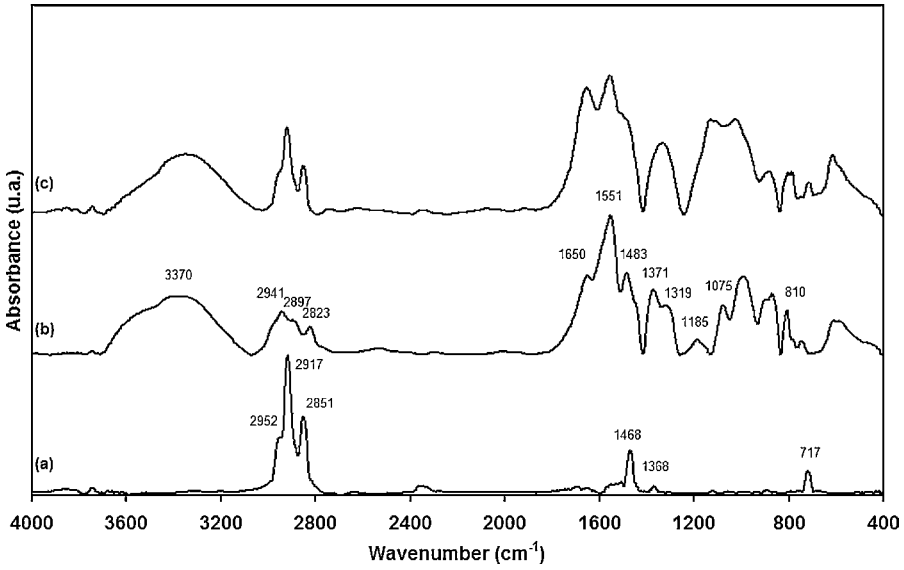

Fig. 3. FT-IR spectra of PCMs formulation (a), melamine–formaldehyde shell (b) and microencapsulated PCMs with melamine–formaldehyde shell (c).

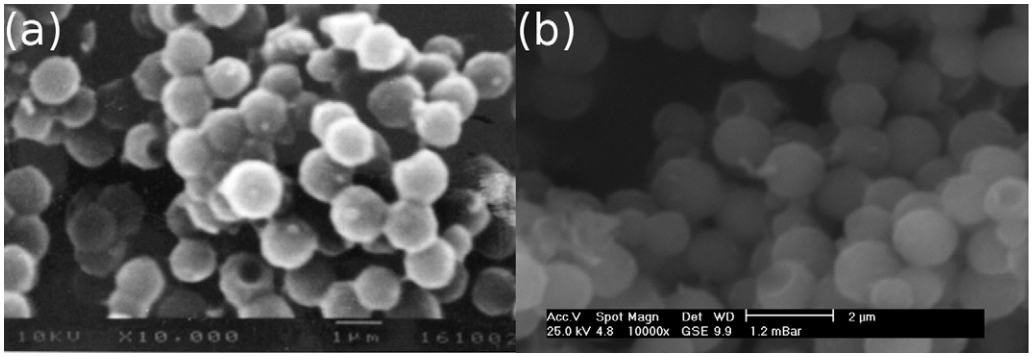

Fig. 4. SEM micrographs of microcapsules with different stirring rates, 10 000 (a) (10 kV, 10 000×) and 13 500 (b) (25 kV, 10 000×), respectively.

hand, C–O–C stretching due to ether bridge at 1075 cm^{-1} is also present. The characteristic absorption bands of aliphatic C–N vibration appeared between 1200 and 1170 cm^{-1}. The absorption peaks of the core material at 2952–2823 cm^{-1}, 1468 cm^{-1}, 1368 cm^{-1}, and 717 cm^{-1} and amino resin can also be clearly distinguished in the spectrum (c), which confirm the encapsulation of the n-alkane binary mixture by melamine–formaldehyde resin [41].

3.1.2. Morphology of microPCMs

Fig. 4 shows a scanning electron micrograph of the microcapsules. The resulting core–shell microcapsules have relatively uniform sizes and a regular spherical shape. No difference on the mean diameter between the two syntheses realized with two different stirring rates applied during the emulsion step is significant. On the other hand, it seems that the stirring rate applied during the emulsion influences the surface of the microcapsules. Thus, a higher stirring promote the formation of smooth surface, whereas a rough surface and the presence of tiny solid particles deposed on it can be observed in Fig. 4(a), due to precipitation of higher molecular weight melamine–formaldehyde pre-polymer in the continuous medium. Furthermore, no destruction of the capsules walls due to mechanical stirring was perceivable.

3.1.3. Phase change properties of microPCMs

The phase change temperature and the latent heat of fusion and crystallization of PCMs formulation and microencapsulated PCMs were obtained using differential scanning calorimeter and presented in Fig. 5. It can be observed (thermogram a) that two strong endothermic peaks appear at 18.51 °C and 26.11 °C, respectively. The first peak is preceded by a shoulder at 11.91 °C. This is due to different stage melting, as different n-alkane fractions are present in this formulation. In our previous work [20], we have attributed the multiple endothermic and exothermic peaks to the solid–solid and the solid–liquid transitions of the paraffin. The total latent heat, 224 J/g, included the solid–solid transitions as well as the solid–liquid one. The onset temperature of the main peak is found at 15.50 °C. Furthermore, 75% of the latent heat of fusion was found in the 15–30 °C range. Therefore, this formulation is quite satisfactory to be used in thermal comfort requirements in textile field. Endothermic and exothermic enthalpy changes of microcapsules are also given in Fig. 5, and measured during their heating and cooling at the rate of 2 °C/min between −30 °C and 50 °C or 60 °C. This thermogram (b) also shows the same transition than the core material, which implies that these materials are chemically inert during the microencapsulation process [8]. Furthermore, the measured PCMs content, according to Eq. (2), in the microcapsules synthesized is approximately 77%, which is slightly higher than the theoretical content (70%), undoubtedly due to the water and formaldehyde releases occurring during the reaction of hydromethyl group of the melamine–formaldehyde resin and the partially removal of surfactant during the washing treatment. Fig. 5(b) also shows that the exothermic phase change temperatures have shifted to higher temperatures, whereas the onset point of the integrated exothermic peak is close to that of the PCMs formulation one. The increase in temperature can be correlated to the low thermal conductivity of the coating material, which affects the heat transfer rate from the outside to the PCMs inside the melamine–formaldehyde shell, and therefore influenced the phase change temperature of the microencapsulated PCMs.

3.1.4. Thermal and mechanical stabilities of microPCMs

Mechanical and thermal stabilities of microcapsules are some of the most important properties to consider in order to introduce them onto textile fabric. The increase of mechanical strength or heat treatments increases the leakage possibility of the core and therefore decreases the thermal properties and the heat-storage capacity. SEM micrographs of heat-treated microPCMS at 150 °C, 160 °C, 180 °C, 190 °C and 200 °C are shown in Fig. 6. Until 160 °C, the morphology change is not significant; on the other hand from

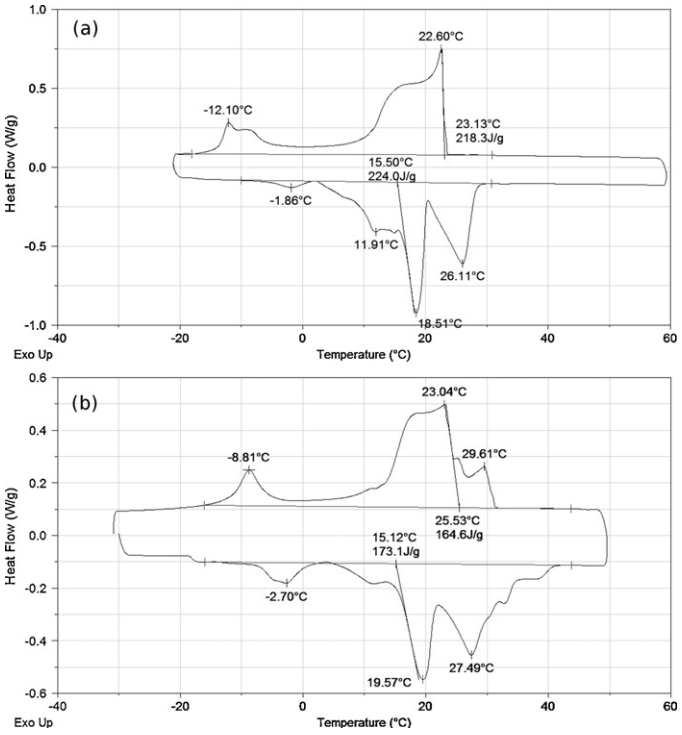

Fig. 5. DSC thermograms of PCMs microcapsules: (a) n-hexadecane/n-eicosane binary mixture and (b) encapsulated PCMs.

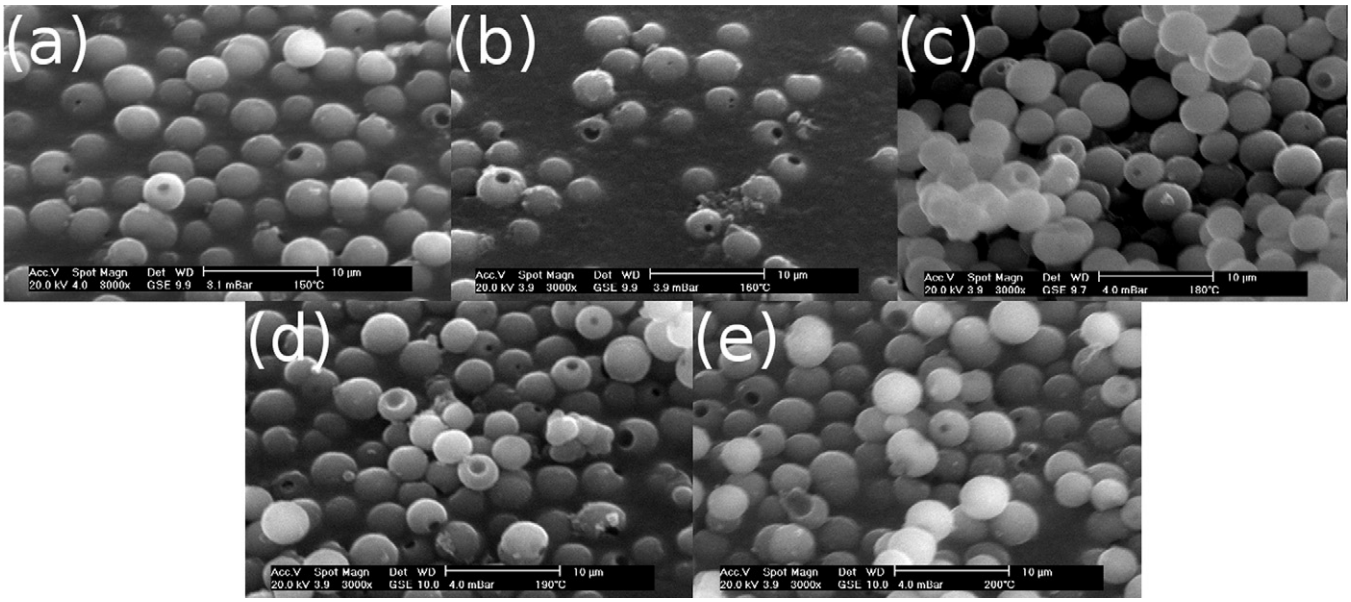

Fig. 6. SEM micrographs of heat-treated microcapsules (20 kV, 3000×): 150 °C (a); 160 °C (b); 180 °C (c); 190 °C (d) and 200 °C (e).

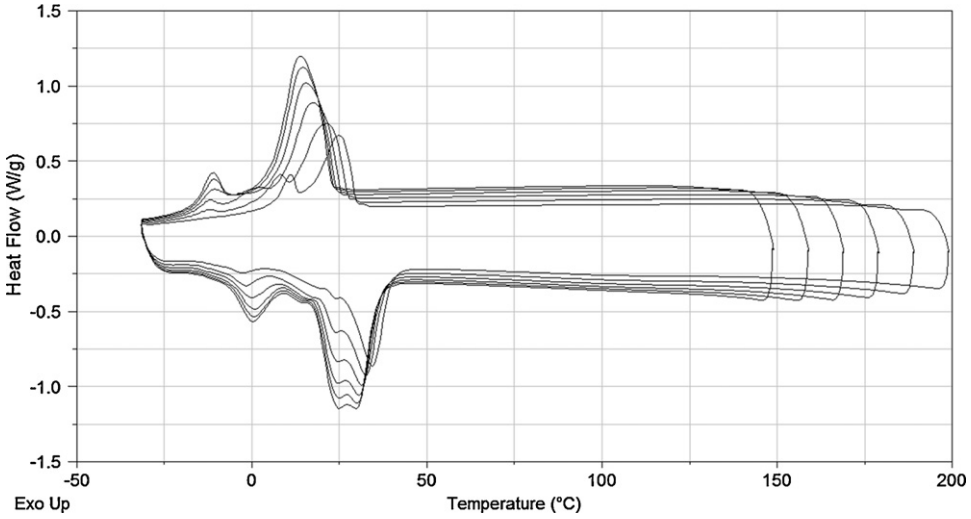

Fig. 7. Thermograms of microPCMs with an isothermal heat treatment at 150 °C, 160 °C, 170 °C, 180 °C, 190 °C, and 200 °C.

160 °C, PCMs diffuse out the particles due to the expansion of one component, n-hexadecane, of the PCMs formulation. Furthermore, even if no thermal decomposition of the amino shell is detected, the surface state presents some orifices which tend to widen with the increase of temperature. In addition, the heat treatment increases the degree of crosslinking of the amino resin from the condensation of the hydroxylmethyl groups, with the elimination of methanol, formaldehyde and water. Therefore, this phenomenon induces the

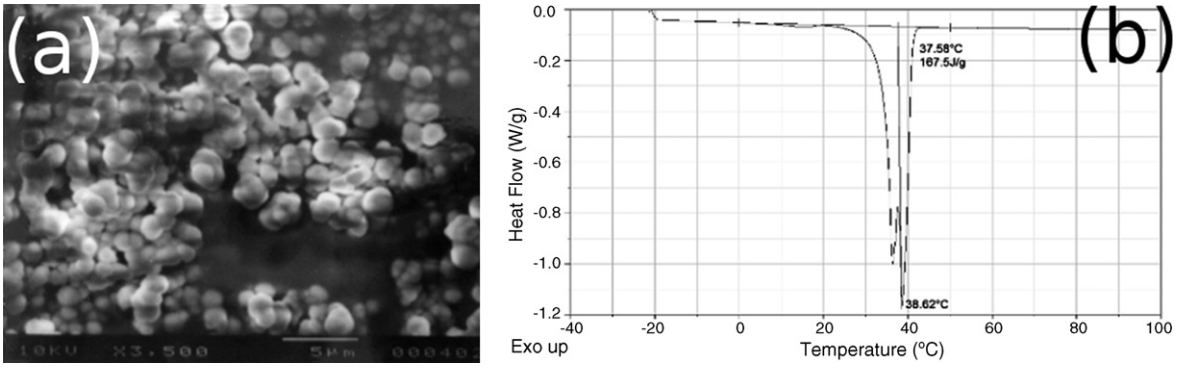

Fig. 8. SEM micrograph (10 kV, 3500×) (a) and thermogram (b) of microcapsules after centrifugation test at 3 × *g* for 60 min.

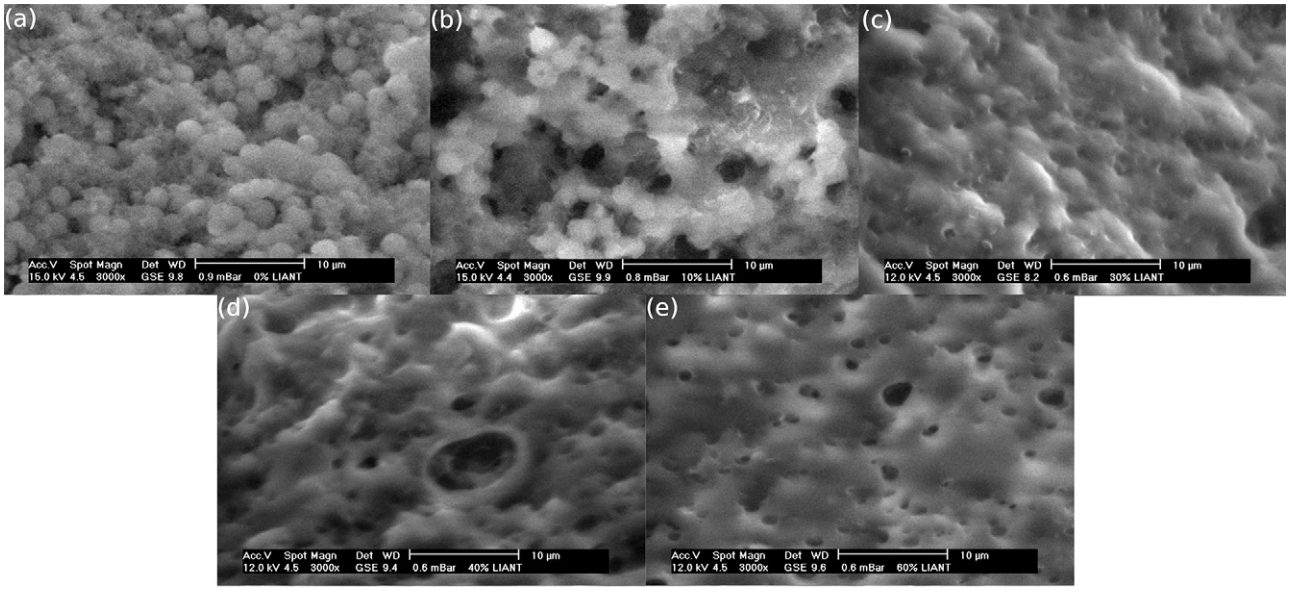

Fig. 9. SEM micrographs of microPCMS/binder films: 100 wt.% microPCMs (a) (15 kV, 3000×); 90/10 wt.% microPCMs/binder (b) (15 kV, 3000×); 70/30 wt.% microPCMs/binder (c) (12 kV, 3000×); 60/40 wt.% microPCMs/binder (d) (12 kV, 3000×); 40/60 wt.% microPCMs/binder (e) (12 kV, 3000×).

shell shrinkage, which allows the diffusion of PCMs out of the particles. The heat treatments are also monitored by DSC (Fig. 7), and it is found that the melting enthalpy of microcapsules decreases with increasing the heat treatment temperature. Thus, the melting enthalpies are found to be equal to 158, 142, 115, 90 and 62 J/g for a temperature of heat treatment of 150 °C, 160 °C, 180 °C, 190 °C and 200 °C, respectively. Furthermore, the DSC curves also show that the main endothermic peak is shifted to the higher temperature, and thus for a heat treatment at 200 °C close to n-eicosane one. Therefore, microcapsules are sensible to the temperature of heat treatment, the thermal properties remain intact until 160 °C; but from 160 °C, n-hexadecane diffuses or degrades first and the loading content decreases.

The mechanical stability is evaluated from centrifugal tests for 1 h in water at 3 × *g*; afterward the phase change properties and the particles morphologies are monitored by DSC and SEM (Fig. 8), respectively. Interestingly, the wall of the microcapsules maintained enough thickness and strength for retaining the spherical shape, even if the particles seem to be deformed under this mechanical strength (Fig. 8(a)). No PCMs droplets have been observed visually, which was confirmed by the latent heat measured by DSC (Fig. 8(b)). Nevertheless, the two main endothermic peaks have been shifted to the higher temperatures close to the n-eicosane melting point. This observation is in accordance with the study of Domańska and Morawski, who have observed that the freezing and melting temperatures at a constant composition increase monotonically with pressure [42]. Therefore, the microcapsules are sufficiently resistant and stable to be applied onto textile fabrics if the temperature does not exceed 150 °C.

3.2. Effect of binder ratio on thermal properties of microPCMs/binder composite

Thermal characteristics of thermoregulated textiles depend on the amount of microcapsules deposited onto them related to the ratio microPCMs/binder composite. The morphology of the surface of the linked microcapsules via PU binder was examined prior to their incorporation onto textile to determine the influence of microPCMs/binder ratio. Fig. 9 shows SEM micrographs of some microPCMs/binder composites films after curing. Differences on the surface were observed from these micrographs. Thus, at low binder amount (Fig. 9(b)), most of microcapsules are coated by PU binder to form an opened cell structure at the surface resulting from the water evaporation during the crosslinking. The increase of the binder amount allows to obtain a more smooth film surface with an amount of still air entrapped in the inner structure. Furthermore, it can be noticed that the size and the number of open cells present on the film surface tend to decrease with increasing binder amount.

In addition, the phase change temperatures and latent heat of these films depend on the binder amount (Figs. 10 and 11). The DSC melting behaviour does not change with the increase of the binder amount; the curve shows the two main endothermic peaks. The

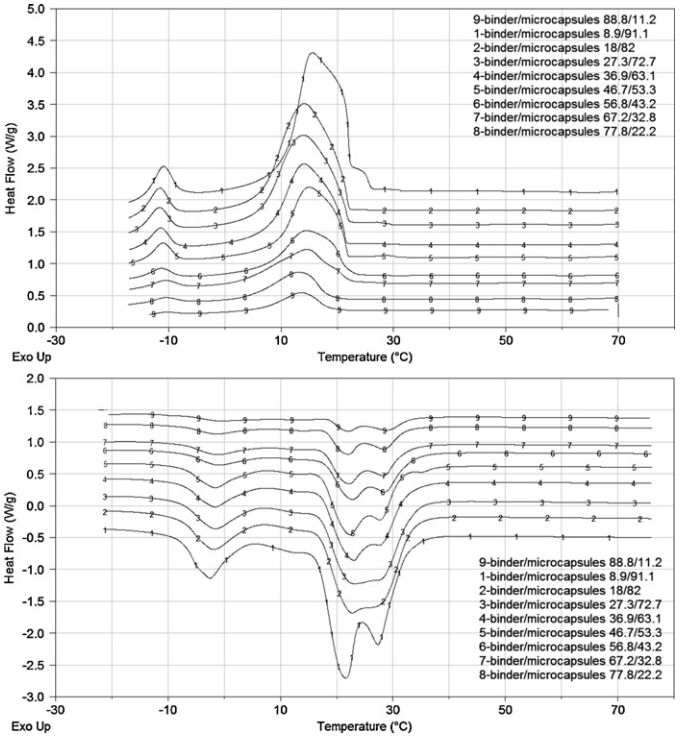

Fig. 10. DSC cooling (a) and heating (b) curves of binder/microcapsules (*x* wt.%/*y* wt.%) composites.

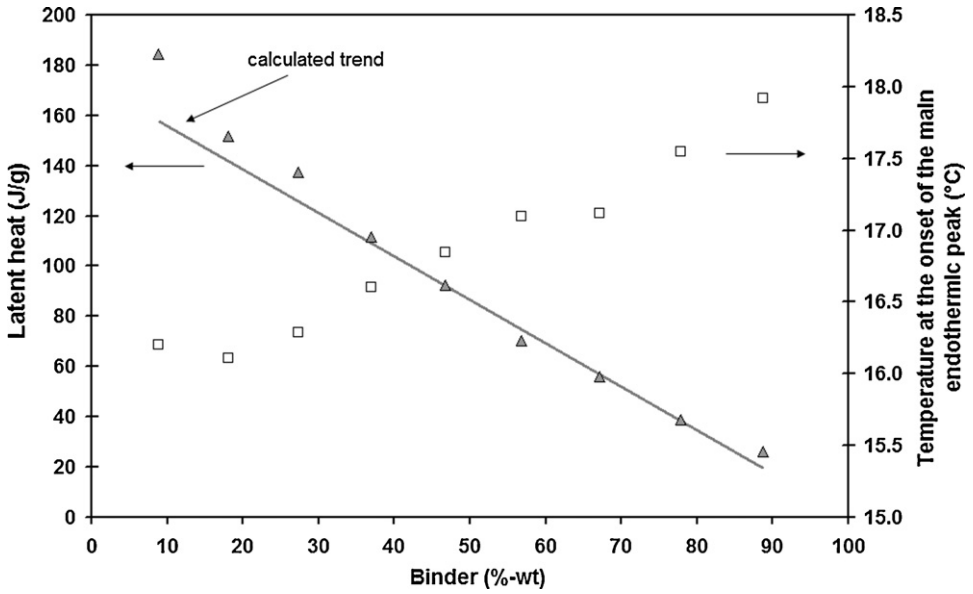

Fig. 11. Influence of the binder amount on the latent heat and the onset temperature of the main endothermic peak.

latent heat measured is close to the theoretical one, even if a light deviation is observed at low binder content. This variation can be due to solvent removal. Interestingly, the onset temperature of the main peak changes according to the binder amount. Thus at low concentration (from 10 to 30 wt.%), it is close to 16 °C, whereas it shifts gradually to the higher temperature underlining the influence of the binder on thermal response of this composite (Fig. 11). The DSC heating scan of the binder used in this study (Fig. 12), a polyester urethane, exhibits an exothermic peak at −38.7 °C, a broad melting endotherm between 0 °C and 30 °C with a melting enthalpy of 23.03 J/g. This exotherm is linked to the soft segment crystallization on heating, whereas the melting endotherm can be associated with crystalline soft segment. It can be noted that crystallization occurs on cooling trace from −7.77 °C. Therefore, this binder is a segmented polyurethane, composed of alternating soft segment, i.e. polyester with low glass transition temperature, and urethane hard segment. Thus, the binder should improve the thermal storage and release properties of the microPCMs/binder composite.

3.3. Properties of treated fabrics

Thermal comfort refers to the state of mind that expresses satisfaction with the thermal environment. The thermal comfort feeling of the human body is influenced by various parameters, in which the thermal properties of clothing materials play an important role. Therefore, it involves the heat transfer between the skin and the environment. The air permeability of the textile is one of the most important factors in thermal comfort. This factor depends mainly upon the construction, the fabric's weight and can vary according to the finishing treatment. The air exchanges are influenced by the microclimate, and then the larger the volume of air participating, the greater the potential for the removal of heat from the wearer. Thus, the manufacture of a thermoregulated textile should be a compromise between the breathability and the thermal transfer of the fabric. Since the structural factors influence the air permeability, the spacing between yarns is one of the main parameters influencing the openness of the treated fabric structure when flow takes place through the inter-yarn pores. The air permeability of the various specimens (Table 2) depends mainly to the binder

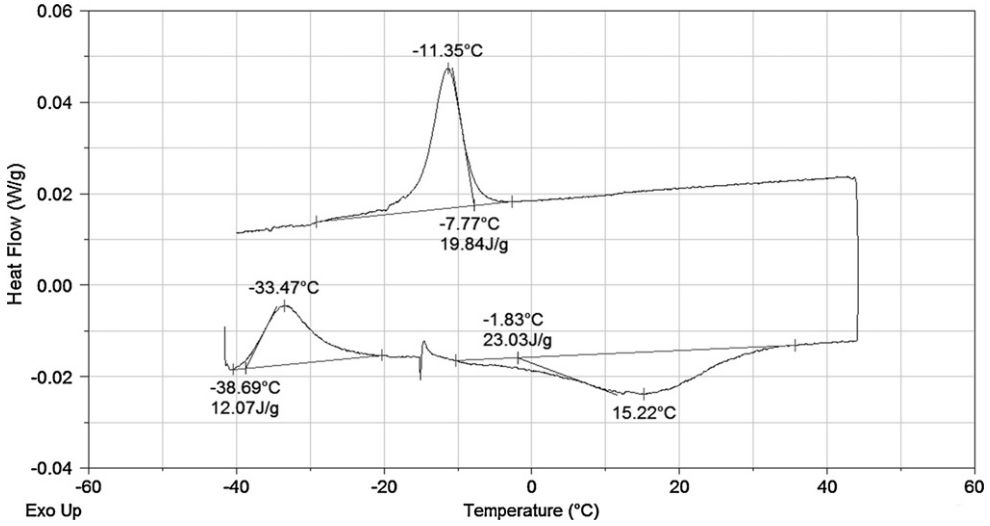

Fig. 12. Thermogram of PU binder.

Table 2
Thermal properties and air permeability of various samples.

Specimen	Add-on (%)	R_{ct}[a] ($m^2\,K\,W^{-1}$)	λ[b] ($W\,m^{-1}\,K^{-1}$)	Air permeability ($l\,m^2\,s$)
COTref	–	0.044	0.20	134.4 ± 5.9
COT1/0-(54)	20.0	0.044	0.19	10.0 ± 6.1
COT1/0-(64)	23.7	0.044	0.19	5.6 ± 1.0
COT1/0-(81)	30.0	0.042	0.20	3.1 ± 0.1
COT4/1-(49)	18.1	0.056	0.18	33.1 ± 0.6
COT3/2-(29)	10.7	0.055	0.19	84.5 ± 6.0
COT3/2-(40)	14.8	0.057	0.17	80.8 ± 0.6
COT3/2-(62)	23.0	0.060	0.16	45.2 ± 4.1
COT2/3-(46)	17.0	0.061	0.19	98.7 ± 7.0
COT1/4-(17)	6.3	0.058	0.17	117.4 ± 3.2
COT1/4-(102)	37.8	0.062	0.15	79.1 ± 2.9
COT0/1-(210)	77.8	0.066	0.18	96.7 ± 11.6

[a] R_{ct} is the total thermal resistance of fabrics.
[b] λ is the thermal conductivity of the fabrics.

amount introduced. The binder coverage and penetration on the fabric surface govern the extent of air permeability. Thus, without microPCMs, air permeability decreases drastically with the increase the binder add-on until obtaining an impermeable substrate. Thus, the binder filled the inter-fibers and the inter-yarn spaces. This is mainly due to the action of the binder that seals the cloth pores of the fabrics, or fills the voids in the space between fibers when it penetrates into the fabric to decrease the air volume though the fabric. Furthermore, a formulation containing only microcapsules results in a decrease of air permeability from 134.4 to 96.7 $l\,m^2\,s$, because the microcapsules fill in the space between fibers and in the space left in the inter-yarn (Fig. 13(a)). As illustrated in Fig. 13(c and d), the coating formulation covers the fabric surface and at high add-on, the voids and interstitial cavities are covered, which decreases the air permeability of the treated fabric. We can also note, that whatever the coating formulation containing microcapsules, the fabric air permeability does not decrease drastically as for samples without microcapsules. Thus, breathability of the fabric is insured by the fact, that the binder links efficiently microcapsules to the fibers rather than to fill the interlaced spaces.

The thermal resistance and conductivity of the treated fabrics with or without microcapsules are shown in Table 2. The differences between the thermal resistances of the various treated fabrics were significant. It was found that as the add-on gets higher the thermal resistance increases whereas the thermal conductivity decreases. On the other hand, as previously observed by Zuckerman et al. [44], the thermal resistance of treated fabrics with PCMs is higher than the one of untreated fabrics. The fact can be correlated to the presence of microcapsules linked in the inter-spaces until to cover the entire fabric surface.

3.4. Thermoregulating response of cotton fabric

In this investigation, PCMs are enclosed in microcapsules and then coated on the surface of cotton fabric to prevent any leakage of the material during the phase change transition. When, the fabric

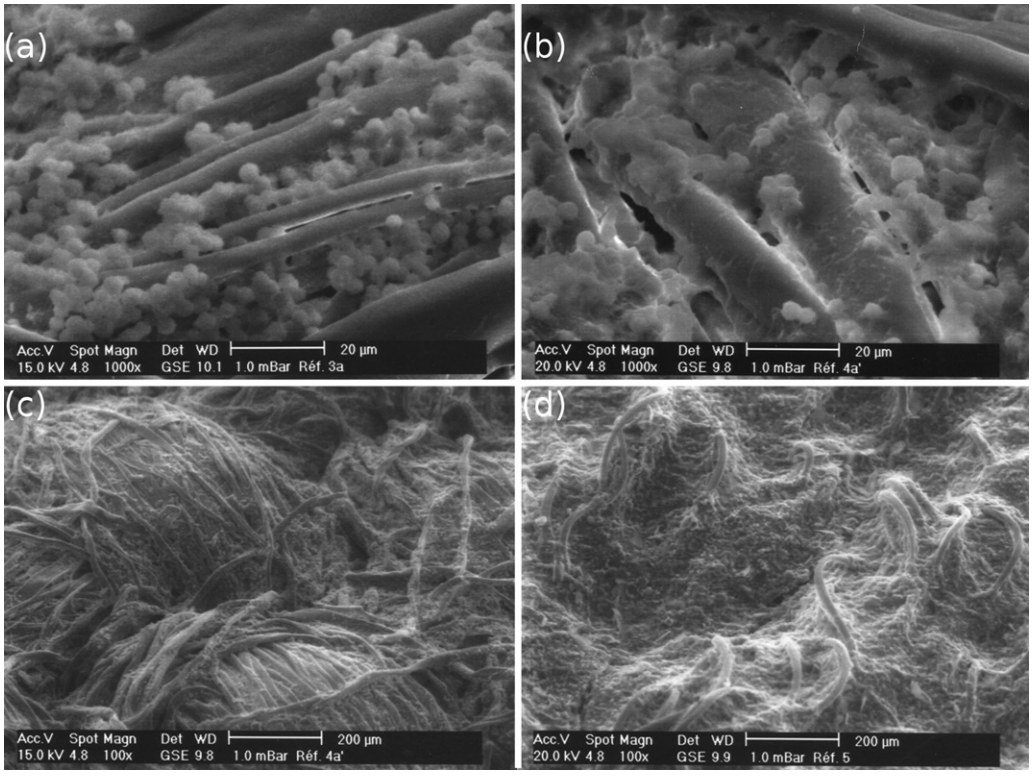

Fig. 13. SEM micrographs of microPCMs treated fabrics: samples COT0/1-(210) (a) (15 kV, 1000×); COT1/4-(61) (b and c) (20 kV, 1000×; 15 kV, 100×); COT1/4-(102) (d) (20 kV, 100×).

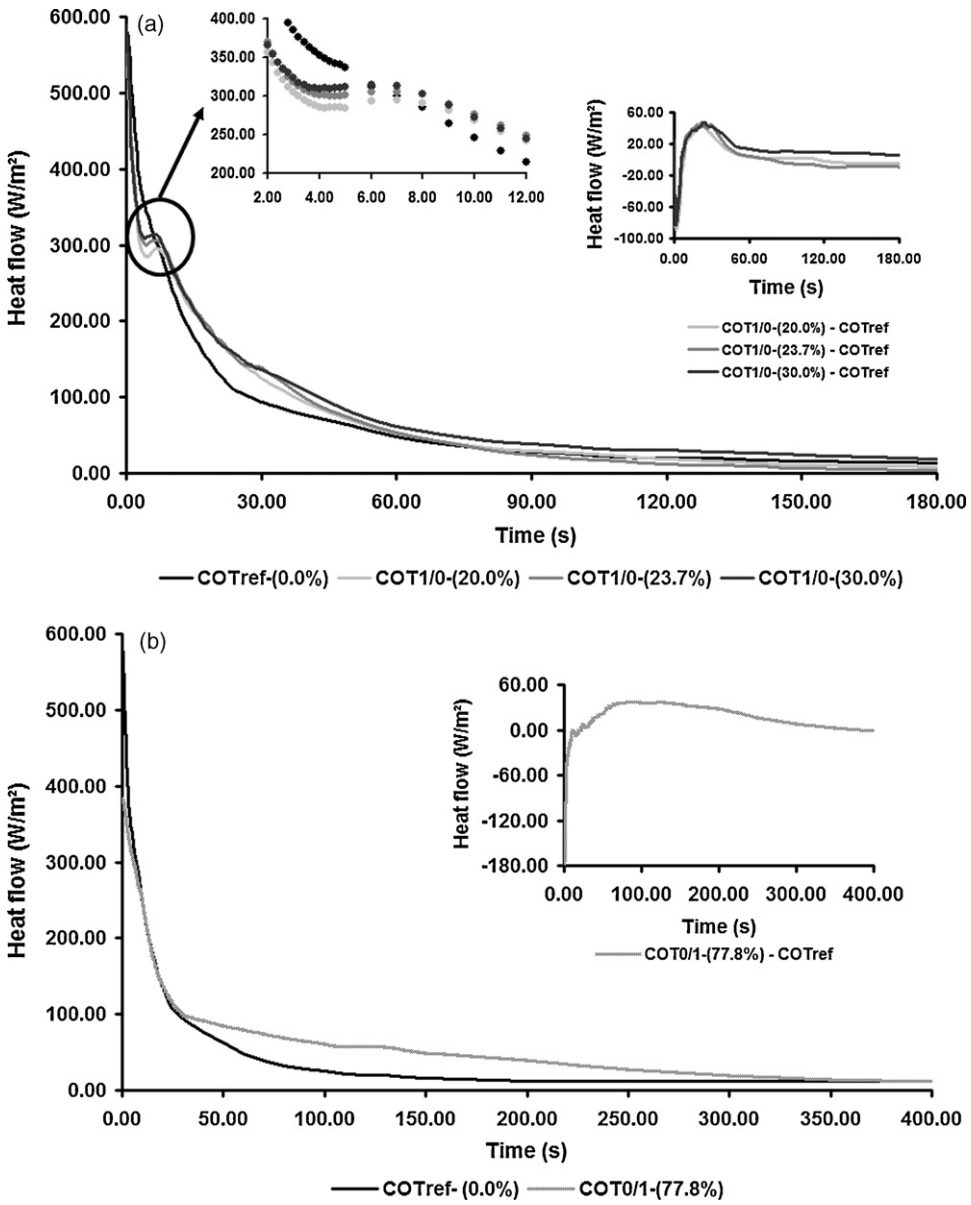

Fig. 14. Variation of heat flow versus time for treated fabrics at different binder amounts (20.0%, 23.7% and 30.0% of add-on) (a) and microcapsules (77.8% of add-on) (b).

is heated, microPCMs can absorb heat energy to go from a solid state to a liquid state producing a cooling effect in the textile layer similar as a buffering effect. In this part, we propose to study the influence of coating formulation, i.e. binder and microPCMs contents, on the thermoregulating response of the treated fabric where the necessary heat to maintain the guarded hot plate at 35 °C is measured during a cold to warm transition.

Thermal characteristics of the fabric would depend mainly on the coating formulation. The influence of binder is shown in Fig. 14(a). Under steady-state conditions, heat data collected are not exactly identical due to the difference between the thermal resistance and conductivity at low temperature. For the samples treated without microPCMs, the heat evolution is composed of four stages:

(1) from 0 to 6 s, the power supply, or the heat loss, is decreasing linearly with a higher slope for binder sample than the reference;
(2) from 6 to 12 s, the curves present a "sinusoidal aspect", due to the melting of the soft segments of the PU binder;
(3) from 12 to 60 s, the heat is decreasing with a lower slope than the first stage; during this stage, the PU binder can store the heat and therefore act as a thermal barrier;
(4) for $t = 60$ s, the heat has reached a steady state.

The difference in heat between the binder layer fabric and the reference is graphed in Fig. 14(a). The response of these samples to a cold to warm transition is interesting to characterize the time lag due to the binder. Of course, the presence of binder allows to delay the heat temperature increase (as long as the temperature varies within the phase change range of the compound).

The difference of heat behaviour between the reference and a sample containing only microPCMs is shown in Fig. 14(b). The heat evolution is divided in two stages, in which firstly, the power supply is decreasing linearly during the first 30 s; and secondly when the temperature in the fabric has reached the phase change temperature of the PCMs, the microPCMs can store the heat which is characterized by a slope lower than the reference's one until the steady state has been reached.

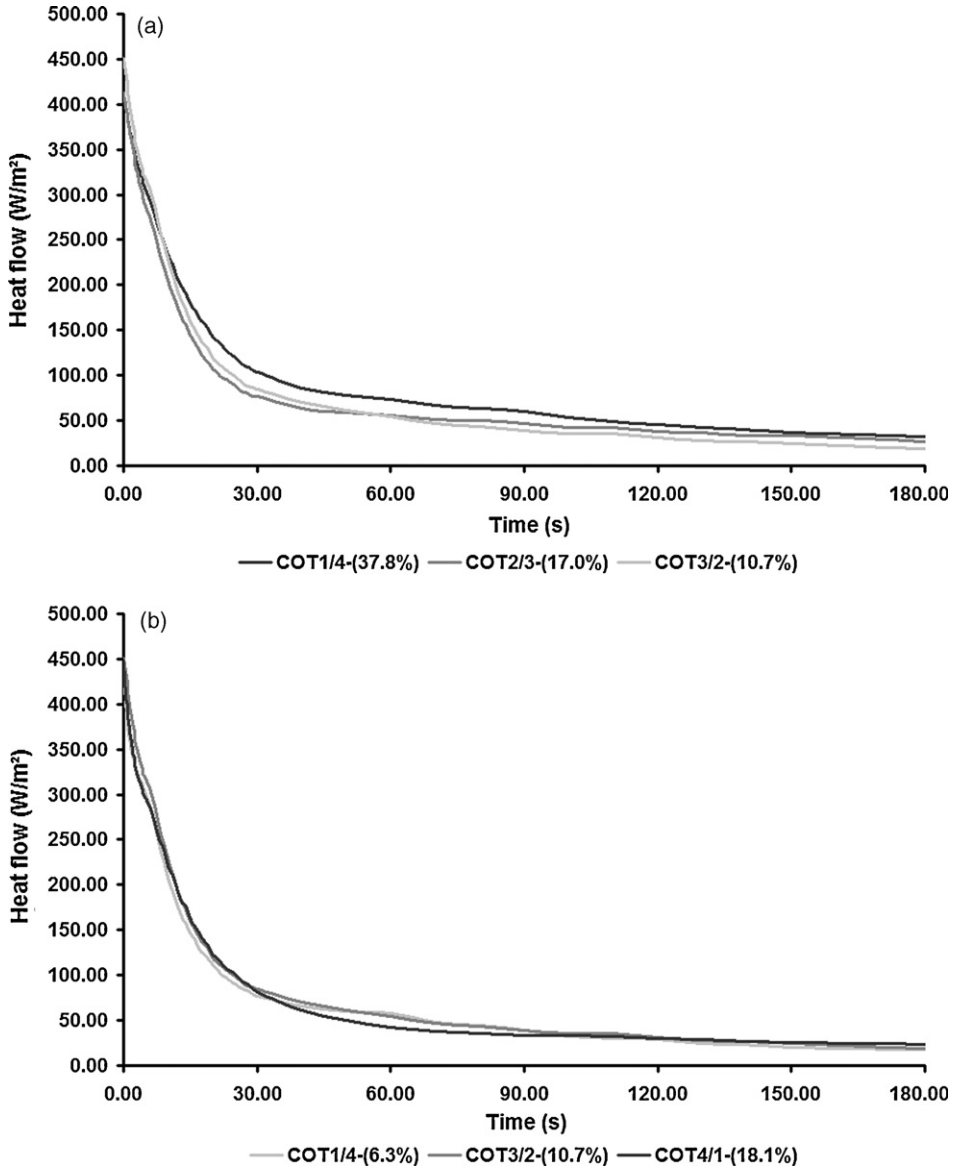

Fig. 15. Variation of heat flow versus time for microPCMs treated fabrics at different binder contents (37.8%, 17.0% and 10.7% of add-on) (a) and microcapsules content (6.3%, 10.7% and 18.1% of add-on) (b).

The influences of microPCMs and binder content on the thermoregulating response of cotton fabric are shown in Fig. 15(a) and (b), respectively. For all the formulation tested with a similar content of binder (~20 g/m^2), the three curves have the same trend. Thus, the heat evolution curves have a break of slope of about 30 s, which corresponds to an outer surface fabric temperature of about 26 °C. From this point, the slopes are much lower when the microPCMs content increases. Furthermore, the changes of heat loss for samples having a low add-on of microPCMs, i.e. 12 g/m^2 and 27 g/m^2 for COT3/2-(29) and COT2/3-(46), respectively, are insignificant; which suggests that the microPCMs effect is compensated by the binder effect. The data collected for the samples (COT3/2-(29, 40, 62)) having the same ratio binder to microPCMs (results do not present) have shown that at low add-on the heat evolution was similar to the reference one, and the cooling buffering effect increased with increasing the add-on. Thus, a minimum add-on related to the ratio binder to microPCMs is required to obtain a cooling effect. On the other hand, COT1/4-(102) shows a good cooling buffering effect until it reaches the steady state from 180 s. For a similar microPCMs content (~10–12 g/m^2) (Fig. 15(b)), the three curves have the same trend until 30 s. From 30 to 120 s, samples with low ratios binder to microPCMs show a better cooling effect. Therefore, the effect of binder is limited from a deposited mass of about 20 g/m^2.

The influence of the starting temperature on the heat evolution is shown in Fig. 16. The sample labelled COT3/2-(62) was studied from a steady state established at 8 °C, 11 °C and 13 °C. The heat variations between the curves at 8 °C and 11 °C are not significant during the first step (from 0 to 16 s) even if the melting phenomenon related previously is more pronounced for the lower temperature. Furthermore, for a starting temperature of 13 °C, this phenomena disappears. The temperature measured on the outer surface versus time varies according the starting temperature. Thus, the data collected for 11 °C and 13 °C are quasi-identical. Beside, for a starting temperature about 8 °C, a shift about 2 °C was observed during the test producing a longer cooling effect until 150 s since more microPCMs were activated. Then, the more heating excitation is rapid, the more the microPCMs textile fabric is efficient for slowing down the temperature increase.

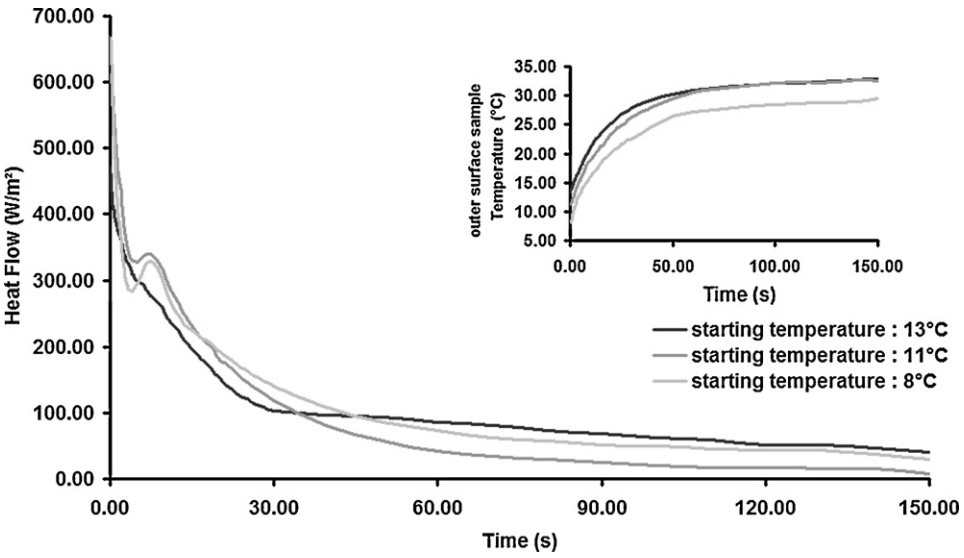

Fig. 16. Influence of the starting temperature on the thermoregulating response of textile fabric (COT3/2-(62), 23% of add-on).

4. Conclusion

MicroPCMs were produced by an *in situ* polymerization process to obtain narrow size particles having a mean diameter within the range of from 1 to 2 μm and containing 77 wt.% of a n-hexadecane/n-eicosane binary mixture in their core. The DSC and MEB investigations have shown that these particles were thermally stable until 160 °C; on the other hand, mechanical stability was also performed furthermore to confirm the possibility to apply them onto textiles substrate by a coating process.

It was found that the thermal behaviour of the microPCMs/binder composites was linked to the thermal properties of the polyurethane binder showing a melting endothermic from 0 °C to 30 °C. Thus, at higher binder content, the main endothermic peak of these composites was shifted to higher temperatures.

When microPCMs were incorporated onto cotton substrate, this textile structure produced a small temporary cooling effect in a transition from a cold environment to a warm environment. Nevertheless, the thermoregulation response depends on the textile properties and more specially on the air permeability modification and the add-on deposited onto the fabric. Furthermore, the results show the preponderant action of the binder during the 30 s when its surface weight deposited was higher than 20 g/m^2. The main contribution of the microPCMs from 30 s appeared from 40 g/m^2, meaning when the outer surface temperature of the textile structure reaches 25 °C; whereas the main endothermic peak of the PCMs formulation was found at 16 °C by DSC measurements. Therefore, during the 30 s, we have obtained a synergetic effect of the binder and the microPCMs limiting the calorific loss due to the modification of the contexture. Thus, a good thermoregulating effect without altering the air permeability property can be obtained for the coating fabrics with 20–40 wt.% of binder related to coating formulation and a minimum of add-on about 17%.

Finally, the cooling effect of our treated textile is more important when the starting temperature is low, which allows to activate both binder and microPCMs containing the n-alkane mixture.

References

[1] G. Nelson, Int. J. Pharm. 242 (2002) 55–62.
[2] D. Aitken, S.M. Burkinshaw, J. Griffiths, A.D. Towns, Rev. Prog. Color. 26 (1996) 1–8.
[3] B. Fei, J.H. Xin, Am. J. Trop. Med. Hyg. 77 (2007) 52–57.
[4] S.K. Ghosh, Functional coatings and microencapsulation: a general perspective, in: S.K. Ghosh (Ed.), Functional Coatings, Wiley-VCH, Weinheim, 2006.
[5] S. Giraud, S. Bourbigot, M. Rochery, I. Vroman, L. Tighzert, R. Delobel, F. Poutch, Polym. Degrad. Stabil. 88 (2005) 106–113.
[6] C.X. Wang, S.H. Chen, J. Ind. Textil. 34 (2005) 157–166.
[7] S. Mondal, Appl. Therm. Eng. 28 (2008) 1536–1550.
[8] N. Sarier, E. Onder, Thermochim. Acta 452 (2007) 149–160.
[9] H. Shim, E.A. McCullough, B.W. Jones, Textile Res. J. 71 (2001) 495–502.
[10] K. Choi, G. Cho, P. Kim, C. Cho, Textile Res. J. 74 (2004) 292–296.
[11] N. Sarier, E. Onder, Thermochim. Acta 454 (2007) 90–98.
[12] X.X. Zhang, X.C. Wang, X.M. Tao, K.L. Yick, Textile Res. J. 76 (2006) 351–359.
[13] Y. Li, Q. Zhu, Textile Res. J. 74 (2004) 447–457.
[14] H. Chung, G. Cho, Textile Res. J. 74 (2004) 571–575.
[15] X.X. Zhang, X.C. Wang, X.M. Tao, K.L. Yick, J. Mater. Sci. 40 (2005) 3729–3734.
[16] B. Pause, US Patent 6,217,993 (2001).
[17] H. Kumano, A. Saito, S. Okawa, S. Takeda, A. Okuda, Int. J. Heat Mass Transfer 48 (2005) 3212–3220.
[18] V. Métivaud, European Thesis, University Bordeaux I, France, 1999.
[19] H. Bo, E.M. Gustafsson, F. Setterwall, Energy 24 (1999) 1015–1028.
[20] F. Salaün, E. Devaux, S. Bourbigot, P. Rumeau, Textile Res. J. 80 (2010) 195–205.
[21] F. Salaün, E. Devaux, S. Bourbigot, P. Rumeau, P.O. Chapuis, S.K. Sahe, S. Volz, Thermochim. Acta 477 (2008) 25–31.
[22] W. Bendkowska, in: H.R. Mattila (Ed.), Intelligent Textiles and Clothing, Woodhead Publishing Ltd, Cambridge, 2006, pp. 34–62.
[23] R. Cox, Chem. Fibers Int. 48 (1998) 475–479.
[24] P. Lennox-Kerr, Techn. Text. Int. 17 (1998) 25–26.
[25] Y.G. Bryant, Techtextil. Symp. 2 (1992) 1–8.
[26] R. Cox, Chem. Fibers Int. 51 (2001) 118–120.
[27] X.Y. Gao, N. Han, X.X. Zhang, W.Y. Yu, J. Mater. Sci. 44 (2009) 5877–5884.
[28] M. Leskovsek, G. Jedrinovic, U. Stankovic-Elseni, Acta Chim. Slov. 51 (2004) 699–715.
[29] N. Sarier, E. Onder, Thermochim. Acta 475 (2008) 15–21.
[30] R.J. Pushaw, US Patent 5,677,048 (1997).
[31] B. Pause, J. Coat. Fabrics 25 (1995) 59–68.
[32] P. Sánchez, M.V. Sánchez-Fernandez, A. Romero, J.F. Rodríguez, L. Sánchez-Silva, Thermochim. Acta 498 (2009) 16–21.
[33] Y. Shin, D. Yoo, K. Son, J. Appl. Polym. Sci. 96 (2005) 2005–2010.
[34] J.H. Kim, G.S. Cho, Textiles Res. J. 72 (2002) 1093–1098.
[35] R. Lottenbach, S. Sutter, WO Patent 02/095314 (2002).
[36] Y.G. Bryant, D.P. Colvin, US Patent 5,499,460 (1996).
[37] J.L. Zuckerman, R.J. Pushaw, B.T. Perry, D.M. Wyner, US Patent 6,207,738 (2001).
[38] P. Monllor, M.A. Bonet, F. Cases, Eur. Polym. J. 43 (2007) 2481–2490.
[39] F. Salaün, E. Devaux, S. Bourbigot, P. Rumeau, Textile Res. J. 79 (2009) 1202–1212.
[40] ISO 9237, Textiles-Determination of the Permeability of Fabrics to Air, 1995.
[41] W. Li, X.X. Zhang, X.-C. Wang, J.-J. Niu, Mater. Chem. Phys. 106 (2007) 437–442.
[42] U. Domańska, P. Morawski, Phys. Chem. Chem. Phys. 4 (2002) 2264–2268.
[43] F. Salaün, E. Devaux, S. Bourbigot, P. Rumeau, Chem. Eng. J. 155 (2009) 457–465.
[44] J.L. Zuckerman, R.J. Pushaw, B.T. Perry, D.M. Wyner, US Patent 6,514,362 B1 (2003).